

TPDM: Selectively Removing Positional Information for Zero-shot Translation via Token-Level Position Disentangle Module

Xingran Chen

University of Michigan
chenxran@umich.edu

Ge Zhang

University of Waterloo
gezhang@umich.edu

Jie Fu*

BAAI
fujie@baai.ac.cn

Abstract

Due to Multilingual Neural Machine Translation’s (MNMT) capability of zero-shot translation, many works have been carried out to fully exploit the potential of MNMT in zero-shot translation. It is often hypothesized that positional information may hinder the MNMT from outputting a robust encoded representation for decoding. However, previous approaches treat all the positional information equally and thus are unable to selectively remove certain positional information. In sharp contrast, this paper investigates how to learn to selectively preserve useful positional information.

We describe the specific mechanism of positional information influencing MNMT from the perspective of linguistics at the token level. We design a token-level position disentangle module (TPDM) framework to disentangle positional information at the token level based on the explanation. Our experiments demonstrate that our framework improves zero-shot translation by a large margin while reducing the performance loss in the supervised direction compared to previous works.

1 Introduction

MNMT systems have been proven to be capable of training on massive language pairs with a single model, and achieving satisfying performance, especially on zero-shot directions (Johnson et al., 2017; Aharoni et al., 2019). Recently, more efforts have been put to further improve the MNMT’s performance by forcing the generation of language-agnostic representation via model modification (Raganato et al., 2021; Gu et al., 2019; Liu et al., 2021; Blackwood et al., 2018; Sachan and Neubig, 2018), data augmentation (Wang et al., 2021; Gu et al., 2019; Zhang et al., 2020), and regularization (Arivazhagan et al., 2019; Al-Shedivat and Parikh, 2019). Besides, prior works have explored

the flaws of existing MNMT models from the perspective of latent variables (Wang et al., 2021; Gu et al., 2019; Liu et al., 2021).

Among these works, Liu et al. (2021) report a counter-intuitive observation that positional information may hinder the encoder from outputting language-agnostic representation due to the different word order of different source languages. To tackle the problem, they remove a residual connection within one layer of the transformer encoder to decrease the contained positional information in representation, thereby improving model performance on zero-shot translation. However, they consider positional information integratedly, leading to the following questions:

- **Q1:** Does MNMT benefit from any part of the positional information?
- **Q2:** If the answer to **Q1** is positive, how much and which part of positional information do we need to improve the zero-shot MNMT performance?

This paper investigates how the positional information influences MNMT performance at the token level. We observe that the vanilla Transformer used for MNMT also learns to disentangle positional information during training, while the Transformer without positional embedding learns to catch positional information during training. We conduct further token-level experiments and propose explanation about the observations accordingly: (1) The word order of some languages is relatively free, meaning that not all positional information is necessary; (2) meanwhile, positional information is needed for sentence-level ordering, as well as for words requiring strict order to disambiguate the semantic meaning (*e.g.*, number). Based on this findings, we conjecture that the token-level positional information disentanglement, where the model can selectively remove positional information, will be

* Corresponding Author

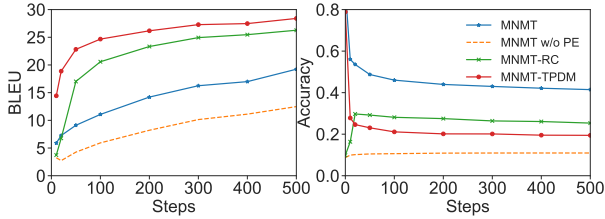


Figure 1: The performance curve of zero-shot translation (left) and positional information probing (right) of different MNMT models.

better for boosting the quality zero-shot translation. To address this, we treat each token’s semantic information and positional information as two separate latent variables and implement disentangled representation learning between them by minimizing their mutual information. Experiments confirm the effectiveness of the proposed approach on improving the zero-shot MNMT performance by a large margin while achieving comparative results on supervised tasks (Liu et al., 2021). Our contributions can be summarized as follows:

- We make an exhaustive study on the specific mechanism of positional information influencing MNMT performance.
- We design an innovative token-level disentangle position module which improves the zero-shot MNMT performance by a large margin while losing less performance on supervised directions than in previous work.
- We conduct detailed ablation experiments to demonstrate the improved robustness of our proposed framework, and justify that our model can selectively remove positional information for tokens.

2 Positional Information Impact Analysis

In this section, we probe the impact of positional information on translation following (Liu et al., 2021). Specifically, we investigate the variation of positional information within the model during training. The probing task aims to detect whether the representation of each token contains information about its corresponding position within the sentence. We choose three models for probing: 1) the vanilla Transformer (denoted as **MNMT**); 2) the residual connection cut mechanism proposed by (Liu et al., 2021) (denoted as **MNMT-RC**); 3) the vanilla Transformer without positional embedding

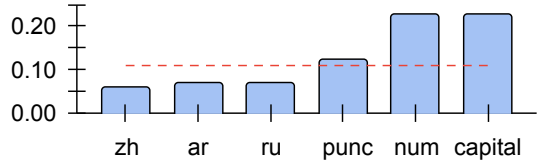


Figure 2: The accuracy of MNMT without PE on the positional information probing task. The results are grouped by the different classes of tokens. The red dotted line indicates the overall accuracy of MNMT without PE on the probing task. Note that *ar*, *zh*, *ru* indicate tokens of Arabic, Chinese, Russian, respectively; *punc* indicates punctuation tokens, *num* indicates number tokens, and *capital* indicates tokens with first letter capitalized.

(denoted as **MNMT without PE**)¹. Experimental details are given in § 4.3. During probing, we freeze all parameters of the MNMT model, and train an MLP to classify the position of each token correctly. Note that we use the zero-shot direction data to train and evaluate the classifier. The results are given in Fig. 1 and Fig. 2.

Surprisingly, as shown in Fig. 1, we observe that although full positional information is provided for MNMT, the accuracy of the probing task is still decreasing during training, meaning that the vanilla Transformer itself is also trying to disentangle positional information during training. Even though no positional information is provided for MNMT without PE, the accuracy of the probing task increases during training. These observations imply that the model keeps trying to learn positional information for achieving better performance. Additionally, MNMT without PE performs poorly both on supervised and zero-shot directions. Similarly, MNMT-RC, which achieves the best zero-shot results, tries to capture positional information in the initial stage of training. These observations indicate that MNMT benefits from optionally introducing position information.

Therefore, to further understand the specific mechanism of positional information influencing MNMT performance, we calculate the probing accuracy for each token within the vocabulary and classify these tokens into various classes based on their semantics. We analyze the probing results of MNMT without PE to investigate which positional

¹We view the baseline MNMT model as the upper bound of the positional information added to the model, and the MNMT without PE model as the lower bound of the positional information added to the model

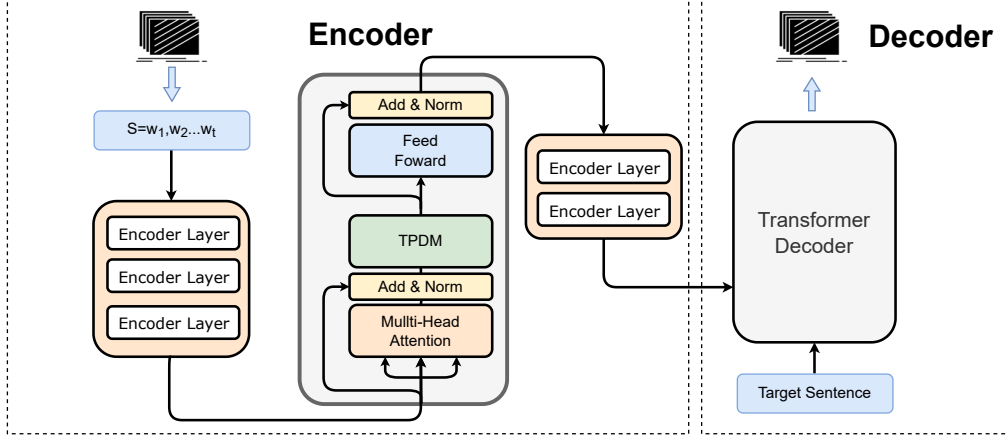


Figure 3: Illustration of our proposed framework MNMT-TPDM. We add the TPDM in an encoder layer within the Transformer to disentangle positional information at the token level. In our experiments, we select 4th for base model and 2nd for small model to add TPDM.

information is automatically learned to improve MNMT performance. As shown in Fig. 2, we observe that the lower bound model 1) learns more positional information on tokens belonging to punctuation, number, and words capitalized in the first letter, but 2) preserve less positional information on Arabic, Chinese and Russian tokens. These results indicate that disentangling positional information is achieved at the token level, and they could be well explained from the perspective of linguistics. Some linguistics research (Comrie et al., 1987; Alasmari et al., 2016; Hoffman, 1996) claims that the word order of some languages is relatively free compared to English. We hypothesize that MNMT should preserve positional information for tokens indicating sentence-level ordering (e.g., capital, punc.), and strict order phrases (e.g., number) to achieve better performance based on these linguistic research.

To fully utilize the token-level positional information for disentanglement, we propose a token-level position disentangle framework to help MNMT learn to disentangle positional information at the token level.

3 Methodology

In this section, we introduce the Token-Level Position Disentangle Module (TPDM) for MNMT to address the problem we discussed in § 2. We set the Transformer as our backbone, and we propose a token-level position disentangle module to add to the model. The illustration of our model is shown in Fig. 3. In § 3.3, we introduce our proposed TPDM and two training objectives for the model and the adversarial generator. § 3.4 describes a training

regularization to make sure that the generated representation of the positional head represents the positional information.

3.1 Preliminary

3.1.1 Transformer

In this paper, we use the Transformer (Vaswani et al., 2017) as our baseline. The Transformer consists of an encoder and a decoder, which are stacks containing n of encoder/decoder block. In this subsection, we will discuss the encoder block in detail. Given an input hidden states H_{i-1} , the i^{th} encoder block first feed its input into a multi-head attention module followed by a residual connection; then, it will be further fed into a feed-forward layer followed by another residual connection. (Liu et al., 2021) introduced an operation to remove the first residual connection in a middle layer m of the Transformer encoder to disentangle the semantic embedding from positional information. We propose TPDM to allow the model to learn to disentangle positional information at the token level.

3.1.2 Disentangle Representation Learning via Minimizing Mutual Information

In disentangling representation learning, given two latent embeddings y and z drawn from the variational distribution $q_{\theta}(y, z|x)$, disentangling y and z can be achieved by minimizing the mutual information $I(y; z)$ between them (Cheng et al., 2020b). However, obtaining a differentiable estimation of mutual information for back-propagation could be intractable (Cheng et al., 2020a), and inaccurate when the dimension increases (Belghazi et al.,

2018). Recently, (Cheng et al., 2020b) proposes an adversarial training-based approach to minimize the upper bound of mutual information instead to decrease the computational difficulty. The proposed sample-based mutual information upper bound is:

$$\hat{I}(\mathbf{y}; \mathbf{z}) = \frac{1}{M} \sum_{j=1}^M \left\{ \log p_{\sigma}(\mathbf{z}_j | \mathbf{y}_j) - \frac{1}{M} \sum_{k=1}^M \log p_{\sigma}(\mathbf{z}_j | \mathbf{y}_k) \right\}, \quad (1)$$

where p_{σ} is a generator that learns the mapping from \mathbf{y} to \mathbf{z} through maximizing $\log p(\mathbf{y} | \mathbf{z})$. Given the upper bound, the disentangle representation learning objective for q_{θ} becomes:

$$\theta^* = \arg \min_{\theta} \hat{I}_{\theta}(\mathbf{y}; \mathbf{z}). \quad (2)$$

Note that the p_{σ} and q_{θ} will be updated alternatively during training. In this paper, we utilize the method to disentangle the positional embedding. First, we treat the encoder of the Transformer as q_{θ} , then we generate two latent embeddings $\mathbf{h}_i, \mathbf{p}_i$ representing semantic and positional information from q_{θ} , to conduct disentangle representation learning.

3.2 Multilingual Neural Machine Translation System

Given a multilingual parallel dataset $\{(\mathbf{x}_k, \mathbf{y}_k, s_k, t_k)\}_{k=1}^D$, where \mathbf{x}_k represents the source text, \mathbf{y}_k represents the target text, and s_k, t_k represents the language ID of \mathbf{x}_k and \mathbf{y}_k , respectively, training a MNMT model with parameters θ involves optimizing the following training objective, where x_k^* is the original sentence started with target language ID token $\langle t_k \rangle$ referring to the initial setting of (Johnson et al., 2017):

$$\mathcal{L}(\theta) = - \sum_{k=1}^D \log p(\mathbf{y}_k | x_k^*; \theta). \quad (3)$$

3.3 Token-Level Position Disentangle Module (TPDM)

We propose a position disentangle module to disentangle positional information at the token level. The detailed illustration of our proposed module is shown in Fig. 4.

Given a token x within a sentence $\mathbf{x} = \{x_1, \dots, x_t\}$, we first view the whole encoder as q_{θ} , and then draw both semantic latent embedding \mathbf{h}_i and positional latent embedding \mathbf{p}_i of token x_i from it. Since the Transformer encoder can only

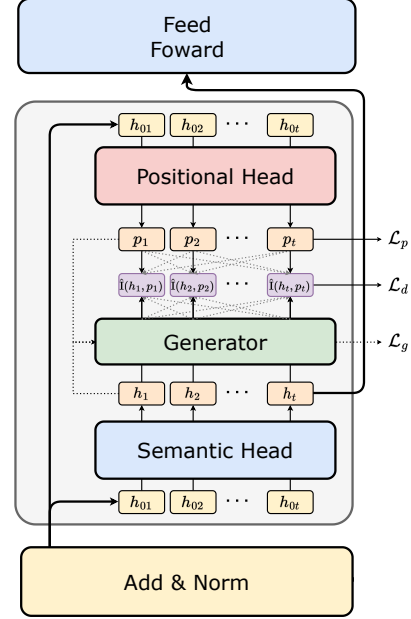


Figure 4: Detailed illustration of the structure of TPDM in Fig. 3. The input is fed into two Siamese MLP heads to generate semantic latent embedding \mathbf{h}_i and positional latent embedding \mathbf{p}_i for each token, respectively. Then token-level mutual information $\hat{I}(\mathbf{h}_i; \mathbf{p}_i)$ is calculated for disentangling the model. The latent semantic embedding \mathbf{h}_i is then viewed as the output of the module to be fed into the feed-forward module.

output a single embedding, to tackle with this problem, inspired by (Li et al., 2021), we propose two siamese MLP heads \mathcal{M}_h and \mathcal{M}_p , which are **not weight shared**, to generate \mathbf{h}_i and \mathbf{p}_i respectively. To be specific, given a hidden states \mathbf{h}_{0i} , we have:

$$\mathbf{h}_i = \mathcal{M}_h(\mathbf{h}_{0i}), \quad (4)$$

$$\mathbf{p}_i = \mathcal{M}_p(\mathbf{h}_{0i}). \quad (5)$$

We aim to minimize the mutual information $I(\mathbf{h}_i, \mathbf{p}_i)$ to disentangle \mathbf{h}_i and \mathbf{p}_i , and Eq. 1 is used to calculate the estimation of $I(\mathbf{h}_i, \mathbf{p}_i)$. Specifically, we define a neural network \mathcal{G}_{σ} with parameters σ to represent the generator p_{σ} . Then, we project \mathbf{h}_i to the embedding space of \mathbf{p}_i utilizing \mathcal{G}_{σ} . Finally, we calculate the conditional probability $p_{\sigma}(\mathbf{p} | \mathbf{h})$ as follow:

$$p_{\sigma}(\mathbf{p}_j | \mathbf{h}_i) = \frac{\text{sim}(\mathcal{G}(\mathbf{h}_i), \mathbf{p}_j) / \tau}{\sum_{k=1}^t \text{sim}(\mathcal{G}(\mathbf{h}_i), \mathbf{p}_k) / \tau}, \quad (6)$$

where $\mathbf{p}_k, \mathbf{p}_j$ belong to tokens x_k, x_j within the sentence, respectively. $\text{sim}(\cdot)$ represents the cosine similarity function, and τ represents the temperature hyper-parameter. During training, given

a mini-batch of data $\{(\mathbf{x}_i, \mathbf{y}_i)\}_{i=1}^b$, we calculate the estimation of mutual information $\hat{I}(\mathbf{h}_{ij}; \mathbf{p}_{ij})$ of each source token x_{ij} respectively. Hence, the disentangle training objective for the whole model, and the training objective for the generator \mathcal{G}_σ are:

$$\mathcal{L}_d(\theta) = \sum_{i=1}^b \sum_{j=1}^t \hat{I}(\mathbf{h}_{ij}; \mathbf{p}_{ij}), \quad (7)$$

$$\mathcal{L}_g(\sigma) = - \sum_{i=1}^b \sum_{j=1}^t \log p_\sigma(\mathbf{p}_{ij} | \mathbf{h}_{ij}). \quad (8)$$

As shown in Fig. 4, the semantic latent embedding h_i of each token will be fed into the feed-forward layer within the encoder layer.

3.4 Regularization of Positional Embedding Head

In this subsection, we introduce a regularization for positional head \mathcal{M}_p to ensure the generated latent positional embedding p_i of \mathcal{M}_p could correctly represent the position of the corresponding input tokens. To address this, an intuitive consideration is that the positional embedding should be example-agnostic. Hence, we follow (Gao et al., 2021; Chen et al., 2020) to maximize agreement among embeddings in the same positions while pushing those that are in different positions away. Formally, given a mini-batch of training examples $\{\mathbf{x}_i, \mathbf{y}_i\}_{i=1}^b$, we set the auxiliary training objective for position alignment as follows:

$$\mathcal{L}_p(\theta) = \sum_{i=1}^b \sum_{j=1}^t -\log \frac{\text{sim}(\mathbf{p}_{ij}, \bar{\mathbf{p}}_j) / \tau}{\sum_{k=1}^t \text{sim}(\mathbf{p}_{ij}, \bar{\mathbf{p}}_k) / \tau} \quad (9)$$

where $\bar{\mathbf{p}}_k = \frac{1}{b} \sum_{i=1}^b \mathbf{p}_{ik}$ represent the contrastive learning anchor of the k^{th} position, τ represents the temperature hyper-parameter.

3.5 Gated Mechanism for Automatic Token-Level Disentanglement

We also try a variant of TPDM, where we introduce a gated mechanism to implement the selective mechanism. To be specific, inspired by (Paranjape et al., 2020), we introduce a learnable mask \mathbf{z} for the MNMT to selectively mask the unnecessary mutual information:

$$\hat{I}'(\mathbf{h}_i; \mathbf{p}_i) = \mathbf{z} \otimes \hat{I}(\mathbf{h}_i; \mathbf{p}_i), \quad (10)$$

where $\mathbf{z} \in \{0, 1\}^t$, and t is the length of input sentence. To obtain a differentiable \mathbf{z} for model

to learn to disentangle at the token-level, we apply a differentiable and continuous binary mask \mathbf{z}^* proposed by (Paranjape et al., 2020) to approximate \mathbf{z} . Therefore, the modified training objective for disentangling becomes:

$$\mathcal{L}'_d(\theta) = \sum_{i=1}^b \sum_{j=1}^t \mathbf{z}^* \otimes \hat{I}(\mathbf{h}_{ij}; \mathbf{p}_{ij}), \quad (11)$$

3.6 Training Objectives

Overall, the training objective of the Transformer model with TPDM is to find parameters θ^* such that:

$$\theta^* = \arg \min_{\theta} (\mathcal{L}(\theta) + \mathcal{L}_d(\theta) + \mathcal{L}_p(\theta)), \quad (12)$$

Note that when the gated mechanism is applied, the $\mathcal{L}_d(\theta)$ in Eq. 12 will be replaced by $\mathcal{L}'_d(\theta)$.

The training objective for the adversarial generator \mathcal{G} is to find parameters σ^* such that:

$$\sigma^* = \arg \min_{\sigma} \mathcal{L}_g(\sigma). \quad (13)$$

Following (Cheng et al., 2020b), for each step in the training process, we first calculate Eq. 8 and update the parameter of \mathcal{G} , then we utilize \mathcal{G} to re-compute the $p_\sigma(\mathbf{p}_{ij} | \mathbf{h}_{ij})$ to calculate Eq. 11. Finally, we use Eq. 12 to update the MNMT model.

4 Datasets and Experiment Setting

This section introduces the selected datasets and the experiment setting.

4.1 Datasets

MultiUN is a widely-used translation corpus from the United Nations (Eisele and Chen, 2010). We select Arabic (Ar), Chinese (Zh), Russian (Ru), and English (En) for our experiment. The Ar, Ru, Zh \leftrightarrow En data are used to train the model, and the Zh \leftrightarrow Ar, Ar \leftrightarrow Ru, Zh \leftrightarrow Ru data are used for evaluating the performance of the models on zero-shot direction translation. We select these three languages (Ar, Ru, Zh), because they represent different language families, increasing the difficulty of the zero-shot MNMT task. Note that the MultiUN is also used for experiments in § 2.

Europarl is a well-known machine translation parallel corpus (Koehn et al., 2005) extracted from the proceedings of the European Parliament. Here we choose German (De), French (Fr), and English (En) for performance measurement. We use De \leftrightarrow En and Fr \leftrightarrow En data to train the model, and Fr \leftrightarrow De is used for the zero-shot direction evaluation.

Task	MultiUN							Europarl					
	Ar→Zh	Zh→Ar	Ar→Ru	Ru→Ar	Zh→Ru	Ru→Zh	Zero. Avg.	Sup. Avg.	De→Fr	Fr→De	Zero. Avg.	Sup. Avg.	
PIV-M (small)	35.0	17.6	24.0	19.4	20.9	33.7	25.1	42.8	24.7	20.0	22.4	30.6	
PIV-M (base)	42.8	22.9	30.4	23.3	28.1	40.8	31.4	48.3	28.0	22.3	25.2	33.5	
MNMT-small	7.2	4.7	4.1	5.4	3.9	7.1	5.4	42.8	15.3	9.4	12.4	30.6	
MNMT-RC-small	10.3	6.9	4.2	6.5	2.8	10.5	6.9	42.5	20.6	4.5	12.6	30.4	
MNMT-TPDM-small	26.2	13.2	18.7	14.3	16.6	26.0	19.2	42.3	21.8	17.9	19.9	30.5	
MNMT-GTPDM-small	28.8	15.0	19.8	16.3	17.3	29.4	21.1	42.1	23.7	19.1	21.4	30.0	
MNMT-base	29.3	15.0	20.9	16.2	18.6	29.4	21.6	48.3	27.4	21.2	24.3	33.5	
MNMT-RC-base	41.0	21.0	29.1	21.7	26.2	40.0	29.8	47.4	29.3	23.2	26.3	32.9	
MNMT-TPDM-base	44.0	22.4	30.7	23.1	27.7	42.7	31.8	47.8	29.2	24.0	26.6	33.0	
MNMT-GTPDM-base	43.7	22.3	30.8	23.4	27.4	43.1	31.8	47.4	29.9	24.3	27.1	32.7	

Table 1: Experimental results on MultiUN dataset and Europarl dataset. The symbol $a \rightarrow b$ indicates the performance of models on translating language a to language b . **Zero. Avg.** represents the average results on all zero-shot direction data; **Sup. Avg.** represents the average results on all supervised-direction data. PIV-M indicates the performance of pivot-based translation using MNMT.

4.2 Baselines

We denote our approach as **MNMT-TPDM**, and the gated variant as **MNMT-GTPDM**. In addition, we compare with the following baselines: First, we follow (Johnson et al., 2017) to set a baseline trained on a vanilla Transformer denoted as **MNMT**. **PIV-M** (Gu et al., 2019) represents pivot-based translation using MNMT. In addition, we compare our approach with removing residual connection operation proposed by (Liu et al., 2021), which we denoted as **MNMT-RC**.

4.3 Experimental Details

In this subsection, we will discuss our experimental settings in detail.

4.3.1 Transformer

In our experiments, we use the same setting as (Vaswani et al., 2017) to set the number of Transformer layer $n_{layer} = 6$, attention head $n_{head} = 8$, and size of dimension $d = 512$. For a comprehensive comparison, we also train a smaller scale of model with $n_{layer} = 3$, $n_{head} = 4$ and $d = 256$. We denote the former one as **base model**, and the latter one as **small model**. Note that we use **base model** to conduct experiments for analysis in § 2.

4.3.2 TPDM

Following (Liu et al., 2021), we choose a middle layer of Transformer to insert proposed TPDM. For the base model, we select the 4th encoder block, while for the small model, we choose the 2nd encoder block to insert the TPDM. During our implementation, we use MLP to implement \mathcal{M}_h and \mathcal{M}_p . In terms of \mathcal{G} , we additionally set an encoder layer of Transformer to contextually learn the mapping from p to h for each token within a sequence.

4.3.3 Hyper-parameter Setting

We apply the same hyperparameter settings for both the small and base models. We follow (Wang et al., 2021) to first tokenize all the data using the `mose` package² (for Chinese, we use the `Jieba`³ toolkit), and then apply Byte Pair-Encoding (BPE) (Sennrich et al., 2016) for 40K operations. We select Adam as our optimizer and choose learning rate $5e-4$, max tokens 8000, warm-up steps 4000, and temperature $\tau = 0.05$ during training to train our model. We update our model for 300k steps on the Europarl dataset, and 500k steps for the MultiUN dataset. During the evaluation, we apply beam search = 5 to generate the target sentence and apply `SacreBLEU` (Post, 2018) as our evaluation metrics to evaluate the models. We use 4 Tesla V100 GPUs to conduct our experiments.

5 Evaluation

5.1 Results

As shown in table 1, our proposed framework observably improves the performance on zero-shot translation. Specifically, the MNMT-TPDM and MNMT-GTPDM significantly outperform the baseline model MNMT, and gains 5.5 and 6.5 BLEU points improvement on average over the MNMT-RC. Note that the performance of MNMT-GTPDM-small is even competitive with the MNMT-base model on MultiUN. Compared to PIV-M, the MNMT-TPDM and MNMT-GTPDM model gains 0.9 and 1.2 BLEU points improvement on average under the base model setting on zero-shot directions. Empirically, we verify that our approach is

²<https://github.com/moses-smt/mosesdecoder>

³<https://github.com/fxsjy/jieba>

capable of improving the MNMT’s performance on zero-shot translation.

Furthermore, our model achieves significant performance improvement on Fr \rightarrow De direction in Europarl, and Ar \rightarrow Zh, Ru \rightarrow Zh translation directions in MultiUN. The finding shows that the MNMT-TPDM has substantial effects on different kinds of directions, even for language pairs that come from different language families. Besides, we notice that although we run for different random seeds, both MNMT and MNMT-RC perform poorly on several directions, especially for the small model.

We find out that this is because MNMT-RC-small often translates into a wrong language (*e.g.*, English), while MNMT-TPDM rarely does. This observation shows that our proposed framework is more robust, especially when the models are small.

As for supervised directions translation, we find out that the degree of performance loss of our proposed MNMT-TPDM on supervised direction is further eased compared to MNMT-RC. One possible explanation can selectively preserve positional information for some key tokens when disentangling. We will discuss this in detail in § 5.2.3.

In terms of the performance between TPDM and GTPDM, we find out that although the GTPDM significantly outperforms the TPDM on small model, it performs competitive when the model becomes larger. We consider that this is because the MNMT-TPDM-base model itself is capable of selectively reserving positional information. We will discuss this in detail in § 5.2.3. Moreover, in supervised direction, GTPDM suffers a more severe performance loss than TPDM. We consider it is reasonable since the gated mechanism (Paranjape et al., 2020) introduces an additional training objective for controlling the masks.

5.2 Discussions

In this subsection, we conduct comprehensive experiments to investigate the effectiveness of our proposed framework in various settings.

5.2.1 Ablation Studies

We first conduct several ablation studies to investigate the importance of each component in our proposed TPDM. To be specific, we try to remove \mathcal{L}_d and \mathcal{L}_p from the training process, and evaluate the model’s performance. Note that \mathcal{L}_g does not influence any parameter within the Transformer model, therefore we do not conduct ablation studies

Task	Europarl + Small Model		
	De \rightarrow Fr	Fr \rightarrow De	Zero. Avg.
MNMT-TPDM w/o \mathcal{L}_d	20.0	16.0	18.0
MNMT-TPDM w/o \mathcal{L}_p	20.6	15.6	18.1
MNMT-TPDM + sinusoidal anchor	22.2	18.0	20.1
MNMT-TPDM	21.8	17.9	19.9

Table 2: Ablation studies of our proposed framework.

Task	Europarl + Small Model			
	De \rightarrow Fr	Fr \rightarrow De	Zero. Avg.	Sup. Avg.
MNMT	15.3	9.4	12.4	30.6
MNMT-TPDM	21.8	17.9	19.9	30.5
MNMT + learnable pos.	9.1	7.5	8.3	30.5
MNMT-TPDM + learnable pos.	22.7	18.7	20.7	30.0

Table 3: Results of learnable positional embedding scenario

on it. Besides, we try to utilize i^{th} sinusoidal positional embedding within the vanilla Transformer as the contrastive anchor \bar{p}_i to compute \mathcal{L}_p . The results is shown in Table 2.

As shown in Table 2, we can find out that removing \mathcal{L}_d or \mathcal{L}_p from the training process will lead to a decrease in the model’s performance. The observation verifies that both \mathcal{L}_d and \mathcal{L}_p is crucial to gain a better performance, and it is crucial to disentangle semantic embedding from **positional information**, but not any other latent embedding. Besides, MNMT-TPDM and MNMT-TPDM + sinusoidal anchor show competitive results, meaning that our approach performs well as long as the contrastive anchors represent the corresponding position correctly.

5.2.2 Learnable Positional Embedding Scenario

We also investigate our proposed framework’s effectiveness in the scenario where we follow BERT (Devlin et al., 2019) to replace sinusoidal positional embedding in the Transformer with a learnable positional embedding. The result in table 3 show that, although the learnable positional embedding baseline reaches a competitive result on supervised-direction translation compared to the fixed counterpart, it cannot generalize well to the zero-shot direction translation task. Our proposed MNMT-TPDM reaches better performance in the zero-shot direction translation. These experimental results clearly demonstrate the robustness and generalization capability of our approach.

5.2.3 Token-Level Disentangling Inspection

In this subsection, we mainly discuss the effect of our proposed framework on token-level positional

	capital	num.	punc.	Ar	Ru	Zh
overall	5.44	3.18	0.25	34.2	37.2	22.1
$\Delta_{acc} > 0$	5.68	3.34	0.37	33.9	40.8	18.5

Table 4: Results of Token-level Disentangle Inspection

information disentanglement, and the advantages of our model compared to previous work.

To investigate the question, based on our analysis for the MNMT without PE in § 2, we conduct token-level probing on both MNMT-RC and MNMT-TPDM models. For this probing task, we focus on tokens that preserve more positional information under our model. To be specific, we measure the proportion of different types of tokens in the entire vocabulary, and the proportion of different types of tokens with $\Delta_{acc} = ACC_{TPDM} - ACC_{RC} > 0$. The result is shown in Table. 4.

According to the results, we find out that: (1) the proportion of punctuation, number, and tokens capitalized with the first letter increase significantly. This shows that our method successfully helps tokens to get access to useful positional information; (2) the proportion of tokens in all languages, except Russian, decreases. We hypothesize that the increase in the proportion of Russian tokens may be partly due to the presence of many capitalized tokens in Russian. In addition, as shown in Fig. 1, our model can disentangle more positional information during training, which leads to a faster convergence during training and better results. We additionally provide some case studies in Appendix A to give an intuitive impression of the observations. From the case studies, we find out that the MNMT-RC conspicuously suffers from the erroneous translation of number, and factual errors caused by the numerical mismatch. One possible reason is that it is due to the neighbor tokens’ influence caused by positional information missing.

6 Related Work

Previous MNMT works have shown prominent capacity in zero-shot direction translation. (Johnson et al., 2017) introduces an artificial language token as an auxiliary input to enable a single model to achieve multiple-pair machine translation and improve the zero-shot translation performance. (Lu et al., 2018) further verifies the massive multilingual translation model’s feasibility, especially in the zero-shot direction. However, there is still room for improvement in these methods. Previous research works (Zhang et al., 2020; Al-Shedivat and

Parikh, 2019; Gu et al., 2019) have pointed out the destabilization and common off-target translation issue in zero-shot translation using the existing models.

Based on these observations, meaningful research works have been published to tackle these issues from three major aspects. First, (Raganato et al., 2021; Gu et al., 2019; Liu et al., 2021; Blackwood et al., 2018; Sachan and Neubig, 2018) introduces innovative structures to learn language-agonistic representation and eliminate the source language-pair related bias. Second, well-designed data augmentation procedures are proposed by (Wang et al., 2021; Gu et al., 2019; Zhang et al., 2020). Third, innovated regularization objectives are tried by existing research work (Arivazhagan et al., 2019; Al-Shedivat and Parikh, 2019). Our work proposes a solution to improve the zero-shot MNMT performance by introducing a token-level position disentangle module. Recently, more work has tried to solve the problem from the latent variable perspective (Gu et al., 2019; Wang et al., 2021). For those that are related to our work, (Liu et al., 2021) views positional information as a latent variable that zero-shot MNMT performance suffers from but leaves a blank of analysis about how positional information influences MNMT, especially in the zero-shot direction, systematically. Our work proposes further analysis and a more efficient mechanism accordingly.

7 Conclusion

The paper analyzes the specific mechanism regarding the influence of positional information on machine translation. We consider that the positional information is optionally needed for the MNMT system. Therefore, we propose TPDM to disentangle positional information at the token level and selectively remove the positional information for MNMT. Our experiments show that our proposed framework outperform MNMT-RC on the zero-shot directions, while reducing the performance loss on the supervised direction. Furthermore, compared to MNMT-RC, our proposed model can disentangle more positional information, leading to a faster convergence during training. Finally, in terms of the removing of token-level positional information, we find out that our proposed method can remove positional information well, while selectively preserve it for tokens indicating sentence-ordering (*e.g.*, capital, punc.), or requiring strict

order (e.g., number).

8 Limitations

The proposed MNMT-TPDM in this paper requires about 1% additional parameters. In addition, multiple training objectives are applied during training. Both of these modifications lead to the increase of algorithmic complexity and computational costs. We have revealed the number of the parameters and the time cost for training the model in Appendix D.

References

- Roei Aharoni, Melvin Johnson, and Orhan Firat. 2019. [Massively multilingual neural machine translation](#). In *Proceedings of the 2019 Conference of the North American Chapter of the Association for Computational Linguistics: Human Language Technologies, Volume 1 (Long and Short Papers)*, pages 3874–3884, Minneapolis, Minnesota. Association for Computational Linguistics.
- Maruan Al-Shedivat and Ankur Parikh. 2019. [Consistency by agreement in zero-shot neural machine translation](#). In *Proceedings of the 2019 Conference of the North American Chapter of the Association for Computational Linguistics: Human Language Technologies, Volume 1 (Long and Short Papers)*, pages 1184–1197, Minneapolis, Minnesota. Association for Computational Linguistics.
- Jawharah Alasmari, J Watson, and ES Atwell. 2016. A comparative analysis between arabic and english of the verbal system using google translate. In *Proceedings of IMAN'2016 4th International Conference on Islamic Applications in Computer Science and Technologies*. Leeds.
- Naveen Arivazhagan, Ankur Bapna, Orhan Firat, Roei Aharoni, Melvin Johnson, and Wolfgang Macherey. 2019. The missing ingredient in zero-shot neural machine translation. *arXiv preprint arXiv:1903.07091*.
- Mohamed Ishmael Belghazi, Aristide Baratin, Sai Rajeshwar, Sherjil Ozair, Yoshua Bengio, Aaron Courville, and Devon Hjelm. 2018. Mutual information neural estimation. In *International conference on machine learning*, pages 531–540. PMLR.
- Graeme Blackwood, Miguel Ballesteros, and Todd Ward. 2018. [Multilingual neural machine translation with task-specific attention](#). In *Proceedings of the 27th International Conference on Computational Linguistics*, pages 3112–3122, Santa Fe, New Mexico, USA. Association for Computational Linguistics.
- Ting Chen, Simon Kornblith, Mohammad Norouzi, and Geoffrey Hinton. 2020. A simple framework for contrastive learning of visual representations. In *International conference on machine learning*, pages 1597–1607. PMLR.
- Pengyu Cheng, Weituo Hao, Shuyang Dai, Jiachang Liu, Zhe Gan, and Lawrence Carin. 2020a. [Club: A contrastive log-ratio upper bound of mutual information](#). In *International conference on machine learning*, pages 1779–1788. PMLR.
- Pengyu Cheng, Martin Renqiang Min, Dinghan Shen, Christopher Malon, Yizhe Zhang, Yitong Li, and Lawrence Carin. 2020b. [Improving disentangled text representation learning with information-theoretic guidance](#). In *Proceedings of the 58th Annual Meeting of the Association for Computational Linguistics*, pages 7530–7541, Online. Association for Computational Linguistics.
- Bernard Comrie et al. 1987. *The world's major languages*. Routledge London, UK.
- Jacob Devlin, Ming-Wei Chang, Kenton Lee, and Kristina Toutanova. 2019. [BERT: Pre-training of deep bidirectional transformers for language understanding](#). In *Proceedings of the 2019 Conference of the North American Chapter of the Association for Computational Linguistics: Human Language Technologies, Volume 1 (Long and Short Papers)*, pages 4171–4186, Minneapolis, Minnesota. Association for Computational Linguistics.
- Andreas Eisele and Yu Chen. 2010. [MultiUN: A multilingual corpus from united nation documents](#). In *Proceedings of the Seventh International Conference on Language Resources and Evaluation (LREC'10)*, Valletta, Malta. European Language Resources Association (ELRA).
- Tianyu Gao, Xingcheng Yao, and Danqi Chen. 2021. [SimCSE: Simple contrastive learning of sentence embeddings](#). In *Proceedings of the 2021 Conference on Empirical Methods in Natural Language Processing*, pages 6894–6910, Online and Punta Cana, Dominican Republic. Association for Computational Linguistics.
- Jiatao Gu, Yong Wang, Kyunghyun Cho, and Victor O.K. Li. 2019. [Improved zero-shot neural machine translation via ignoring spurious correlations](#). In *Proceedings of the 57th Annual Meeting of the Association for Computational Linguistics*, pages 1258–1268, Florence, Italy. Association for Computational Linguistics.
- Beryl Hoffman. 1996. [Translating into free word order languages](#). In *COLING 1996 Volume 1: The 16th International Conference on Computational Linguistics*.
- Melvin Johnson, Mike Schuster, Quoc V. Le, Maxim Krikun, Yonghui Wu, Zhifeng Chen, Nikhil Thorat, Fernanda Viégas, Martin Wattenberg, Greg Corrado, Macduff Hughes, and Jeffrey Dean. 2017. [Google's multilingual neural machine translation system: Enabling zero-shot translation](#). *Transactions of the Association for Computational Linguistics*, 5:339–351.

- Philipp Koehn et al. 2005. Europarl: A parallel corpus for statistical machine translation. In *MT summit*, volume 5, pages 79–86. Citeseer.
- Haoyang Li, Xin Wang, Ziwei Zhang, Zehuan Yuan, Hang Li, and Wenwu Zhu. 2021. Disentangled contrastive learning on graphs. *Advances in Neural Information Processing Systems*, 34.
- Danni Liu, Jan Niehues, James Cross, Francisco Guzmán, and Xian Li. 2021. [Improving zero-shot translation by disentangling positional information](#). In *Proceedings of the 59th Annual Meeting of the Association for Computational Linguistics and the 11th International Joint Conference on Natural Language Processing (Volume 1: Long Papers)*, pages 1259–1273, Online. Association for Computational Linguistics.
- Yichao Lu, Phillip Keung, Faisal Ladhak, Vikas Bhardwaj, Shaonan Zhang, and Jason Sun. 2018. [A neural interlingua for multilingual machine translation](#). In *Proceedings of the Third Conference on Machine Translation: Research Papers*, pages 84–92, Brussels, Belgium. Association for Computational Linguistics.
- Bhargavi Paranjape, Mandar Joshi, John Thickstun, Hannaneh Hajishirzi, and Luke Zettlemoyer. 2020. [An information bottleneck approach for controlling conciseness in rationale extraction](#). In *Proceedings of the 2020 Conference on Empirical Methods in Natural Language Processing (EMNLP)*, pages 1938–1952, Online. Association for Computational Linguistics.
- Matt Post. 2018. [A call for clarity in reporting BLEU scores](#). In *Proceedings of the Third Conference on Machine Translation: Research Papers*, pages 186–191, Brussels, Belgium. Association for Computational Linguistics.
- Alessandro Raganato, Raúl Vázquez, Mathias Creutz, and Jörg Tiedemann. 2021. [An empirical investigation of word alignment supervision for zero-shot multilingual neural machine translation](#). In *Proceedings of the 2021 Conference on Empirical Methods in Natural Language Processing*, pages 8449–8456, Online and Punta Cana, Dominican Republic. Association for Computational Linguistics.
- Devendra Sachan and Graham Neubig. 2018. [Parameter sharing methods for multilingual self-attentional translation models](#). In *Proceedings of the Third Conference on Machine Translation: Research Papers*, pages 261–271, Brussels, Belgium. Association for Computational Linguistics.
- Rico Sennrich, Barry Haddow, and Alexandra Birch. 2016. [Neural machine translation of rare words with subword units](#). In *Proceedings of the 54th Annual Meeting of the Association for Computational Linguistics (Volume 1: Long Papers)*, pages 1715–1725, Berlin, Germany. Association for Computational Linguistics.
- Ashish Vaswani, Noam Shazeer, Niki Parmar, Jakob Uszkoreit, Llion Jones, Aidan N Gomez, Łukasz Kaiser, and Illia Polosukhin. 2017. Attention is all you need. In *Advances in neural information processing systems*, pages 5998–6008.
- Weizhi Wang, Zhirui Zhang, Yichao Du, Boxing Chen, Jun Xie, and Weihua Luo. 2021. [Rethinking zero-shot neural machine translation: From a perspective of latent variables](#). In *Findings of the Association for Computational Linguistics: EMNLP 2021*, pages 4321–4327, Punta Cana, Dominican Republic. Association for Computational Linguistics.
- Biao Zhang, Philip Williams, Ivan Titov, and Rico Sennrich. 2020. [Improving massively multilingual neural machine translation and zero-shot translation](#). In *Proceedings of the 58th Annual Meeting of the Association for Computational Linguistics*, pages 1628–1639, Online. Association for Computational Linguistics.

Task	MultiUN														
	Ar→En	En→Ar	Ru→En	En→Ru	Zh→En	En→Zh	Supervised Avg.	Ar→Zh	Zh→Ar	Ar→Ru	Ru→Ar	Zh→Ru	Ru→Zh	Zero-shot Avg.	
MNMT-small	48.1	32.5	45.6	36.3	43.2	51.2	42.8	7.2	4.7	4.1	5.4	3.9	7.1	5.4	
MNMT-RC-small	47.7	32.1	45.1	36.0	42.8	51.1	42.5	10.3	6.9	4.2	6.5	2.8	10.5	6.9	
MNMT-TPDM-small	47.7	31.9	45.3	35.7	42.7	50.6	42.3	26.2	13.2	18.7	14.3	16.6	26.0	19.2	
MNMT-GTPDM-small	47.5	31.9	45.0	35.6	42.3	50.4	42.1	28.8	15.0	19.8	16.3	17.3	29.4	21.1	
MNMT-base	53.9	36.7	50.1	42.2	49.9	57.1	48.3	29.3	15.0	20.9	16.2	18.6	29.4	21.6	
MNMT-RC-base	52.9	36.2	49.5	41.0	48.8	56.0	47.4	41.0	21.0	29.1	21.7	26.2	40.0	29.8	
MNMT-TPDM-base	53.2	36.4	49.7	41.7	49.3	56.7	47.8	44.0	22.4	30.7	23.1	27.7	42.7	31.8	
MNMT-GTPDM-base	53.3	36.1	49.7	40.8	48.6	56.1	47.4	43.7	22.3	30.8	23.4	27.4	43.1	31.8	

Table 6: Full experimental results of MultiUN.

Task	Europarl								
	De→En	En→De	Fr→En	En→Fr	Supervised Avg.	De→Fr	Fr→De	Zero-shot Avg.	
MNMT-small	30.3	24.6	33.8	33.7	30.6	15.3	9.4	12.4	
MNMT-RC-small	30.3	24.3	33.6	33.5	30.4	20.6	4.5	12.6	
MNMT-TPDM-small	30.4	24.2	33.7	33.5	30.5	21.8	17.9	19.9	
MNMT-GTPDM-small	29.7	23.8	33.3	33.0	30.0	23.7	19.1	21.4	
MNMT-base	33.7	27.1	36.7	36.3	33.5	27.4	21.2	24.3	
MNMT-RC-base	32.9	26.4	36.3	35.9	32.9	29.3	23.2	26.3	
MNMT-TPDM-base	33.0	26.6	36.1	36.0	33.0	29.2	24.0	26.6	
MNMT-GTPDM-base	32.9	26.0	35.9	35.9	32.7	29.9	24.3	27.1	

Table 7: Full experimental results of Europarl.

	#Parameters	Time Cost
MNMT-small	30.781M	1.0×
MNMT-TPDM-small	31.046M	1.46×
MNMT-base	94.642M	1.0×
MNMT-TPDM-base	95.696M	1.35×

Table 8: Statistics of the number of parameters and time cost.

D Efficiency of TPDM

In this section, we reveal the difference in parameter and training cost in terms of our proposed MNMT-TPDM. The statistics are shown in Table 8. From the table, the parameters of our proposed MNMT-TPDM have no more than 1% increase on both base and small version of models. In terms of time cost, the training time of our proposed model is increased by around 40%. This is mainly due to the adversarial training procedure.